



Study The Structural and Optical Properties of Sn_{1-x}Cu_xO₂ Thin Films Prepared by Chemical Spray Pyrolysis Method

3086

Aymen G. Hasan*, Ziad T. Khodair and Ammar A. Habeeb

^{1,2,3}Department of Physics, College of Science, University of Diyala, Diyala, Iraq.

Corresponded Author : Aymen G. Hasan: Email: aimanjamhoo@gmail.com

ABSTRACT

Chemical spray pyrolysis is employed in this study to synthesize Sn_{1-x}Cu_xO₂ films with x = 0, 0.03, 0.05, 0.07, and 0.09. XRD is used to investigate structural properties, while UV-VIS-NIR spectroscopy is used to study optical properties. The Scherer formula was used to calculate crystallite size, which showed that it decreased as the copper oxide level increased. The absorption coefficient, extinction coefficient, imaginary and real parts of dielectric constants, and other properties of undoped and doped oxide thin films were investigated. As the percentage of Copper oxide rose, the transmittance of all samples increased as the wavelength of (300 - 500) nm increased. As the copper oxide level grew, the band gap values fell.

Keywords: SnO₂, chemical spray pyrolysis, thin films, Structural Properties.

DOI Number: 10.14704/nq.2022.20.6.NQ22309

NeuroQuantology 2022; 20(6) 3086-3091

1. INTRODUCTION

Transparent conducting oxides (TCOs), including CdO, SnO₂, and In₂O₃, as well as its ternary and more complicated alloys, have piqued researchers' interest over the last two decades. The best compelling motivation to reading TCOs is the increasing number of applications containing the great flat-screen high-definition televisions (HDTVs including liquid crystal display (LCD), plasma and organic light-emitting diode (OLED) based displays), large and high resolution flat screens for portable computers, the energy-efficient low-emittance windows, solar control and electrochromic windows, thin film photovoltaic, oxide based transistors and transparent electronic as well as hand held, flexible and smart devices[1- 4]. For both practical and basic reasons, copper(II)-oxide nanoparticles, which belong to the monoclinic structural system, have sparked interest in recent years. Because of their physical and chemical features, such as superconductivity, photovoltaic capabilities, low cost, and antibacterial activities [5, they have a diverse range of uses. The goal of this study is to use a chemical spray pyrolysis approach to create Sn_{1-x}Cu_xO₂ films, and then analyze their structural and optical features.

2. EXPERIMENTAL DETAILS

Chemical spray pyrolysis method is utilized to synthesize Sn_{1-x}Cu_xO₂ films at x = 0, 0.03, 0.05, 0.07 and 0.09 using high purity materials: (i) Tin chloride (SnCl₄.5H₂O) (99.0%), (ii) Copper Chloride (CuCl₂.2H₂O) (99%). The solutions are prepared by dissolving the amount of (SnCl₄.5H₂O powder with 1 Molarity and amounts of CuCl₂.2H₂O powder with 1 Molarity in distilled waters. Other conditions such as spray distance (29±1) cm, Spraying Rate (60 s), Spraying time (10 s), the temperature of the substrate at 400 °C and the pressure of the carrier gas is (1.6) bar were kept constant for all films. Glass substrates with diameters of (22) cm² are being deposited by thin films. The produced samples' thickness is measured using a gravimetric method and equals (350) nm. The optical properties of the generated samples are studied using UV-VIS-NIR spectroscopy (Shimadzu, UV/1800) and X-ray diffraction (Shimadzu XRD/6000) copper target (Cu-K/ 1.5418 Å).

3. RESULTS AND DISCUSSIONS

3.1. Results of XRD

Figure 1 shows the XRD results of Sn_{1-x}Cu_xO₂ for x = 0, 0.03, 0.05, 0.07, and 0.09. 2 have values of 26° ,



33°, 37°, 51°, 61° and 65°, which correspond to the (110), (101), (200), (211), (310), and (301) favored planes, respectively, and suggest Sn_{1-x}Cu_xO₂ in accordance with the JCPDS card number 00-046-1088. The strongest peak is found at 226°, which is referred to as the (110) plane, which is consistent with the findings of report [2, 3]. The presence of many diffraction peaks and the placements of the peaks led to the conclusion that the films are

polycrystalline and tetragonal in nature. As the amount of Copper oxide is increased, the peak intensity drops. XRD revealed the disappearance of new peaks as the proportion of copper oxide increased, as well as the absence of any residues of copper oxide.

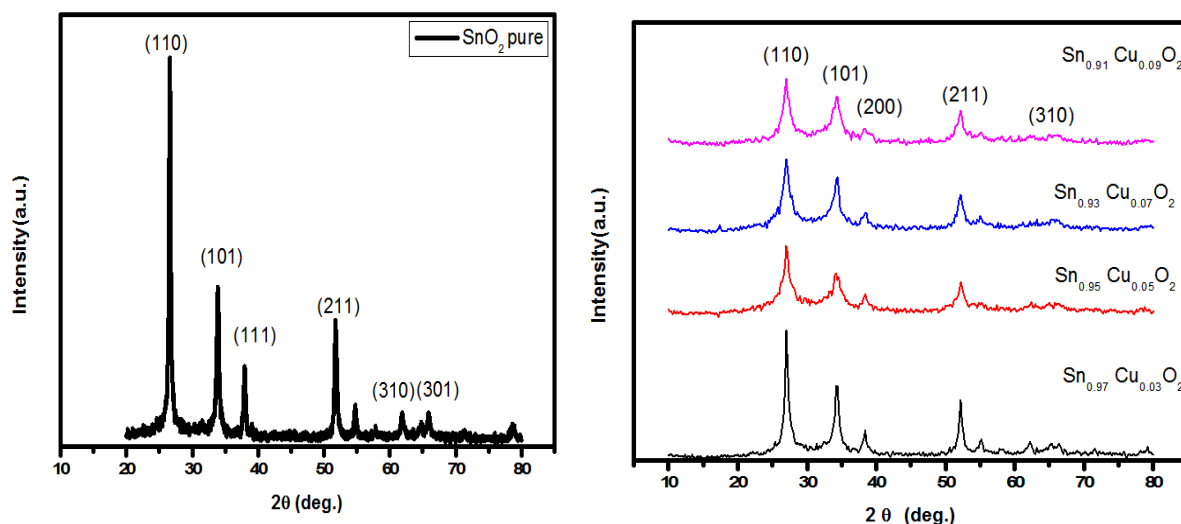


Fig.1: XRD patterns of the Sn_{1-x}Cu_xO₂ at (x= 0, 0.03, 0.05, 0.07 and 0.09).

$$T_C(h, k, l) = \frac{I_{(h, k, l)} / I_{0(h, k, l)}}{N_r^{-1} \sum I_{(h, k, l)} / I_{0(h, k, l)}} \quad \text{Scherer's formula [6- 13] is used to}$$

estimate the average crystallite size for the (110) plane.

$$D_{av} = \frac{K \lambda}{\beta \cos \theta} \quad (1)$$

Where K is factor 0.9, λ is the wavelength of x-ray 1.5406 Å, β is the full width of half maximum of peaks (FWHM), and θ is the angle, Bragg. Table 1 shows that when Copper oxide concentration increases, the average crystallite size decreases, with a value of (28- 9.6), which is consistent with previous results [2, 5]. Micro straining in the structure crystal caused by defects like location and twinning could also cause the peak to broaden. The density of dislocation (δ) is estimated by [6, 9].

$$\delta = \frac{1}{D_{av}^2} \quad (2)$$

As shown in table 1, the size of crystallites and the density of dislocations have an inverse relationship, with the size of crystallites decreasing as the density of dislocations increases and vice versa.

The number of the crystallites (N_o) can be valued by [8, 11]:

$$N_o = \frac{(t)}{D_{av}^3} \quad (3)$$

Where t: the thickness of samples (350 nm). It can be seen that as the Copper oxide ratio increases, the number of crystallites for thin films increases due to an increase in the size of crystallites. The Texture coefficient T_c can be estimated by [9, 10]:

(4) Where the (I_(h,k,l)) is the measured intensity, (I_{o (h,k,l)}) is taken from ICDD data, N is the number of reflections, and hkl is the Miller indices. The (T_c) value is used to define the preferred orientations (hkl) for crystal formation in polycrystalline thin films, as shown in table1. It's worth noting that the (T_c) value is greater than one, indicating that there is more grains in a given (hkl) direction. The preferred development of crystallites in the direction perpendicular to hkl planes increased as T_{c(hkl)} decreased as the copper oxide ratio decreased [7].



Table1, Result of XRD of the strongest three peaks for (Sn_{1-x}Cu_xO₂) at (x= 0, 0.03, 0.05, 0.07 and 0.09).

| 2θ (Deg.) | FWHM (Deg.) | d _{hkl} Exp.(Å) | D _{ave} (nm) | hkl | T _c | δ(line. cm ⁻²) *10 ⁺¹⁸ | N _o (cm ⁻²) *10 ⁺¹⁸ |
|-----------|-------------|--------------------------|-----------------------|-----|----------------|---|---|
| 26.6316 | 0.2913 | 3.3445 | 28.0 | 110 | 2.8 | 12.73 | 159 |
| 27.034 | 0.571 | 3.2956 | 14.3 | 110 | 2.4 | 48.83 | 1194 |
| 27.023 | 0.811 | 3.2969 | 10.1 | 110 | 1.8 | 98.52 | 3422 |
| 27.004 | 0.847 | 3.2992 | 9.6 | 110 | 1.6 | 107.47 | 3899 |
| 27.005 | 0.815 | 3.2991 | 10.0 | 110 | 1.2 | 99.50 | 3474 |

3.2 Optical properties

When employing UV-Vis spectrophotometers, the optical spectra of all films are studied in the range of spectral (300–900) nm. To obtain precise information on the optical energy gap of films, and analysis of the dependence of the coefficient of absorption on photon energy in the vast absorption area was carried out [6, 8]. At various values of x, Fig. (2) depicts the relationship between transmittance and wavelength of Sn_{1-x}Cu_xO₂ films. It is apparent that when the wavelength of (300 - 500) nm increases, the transmittance of all samples increases. The transmittance of thin films increases as the copper oxide ratio increases. The absorbance (A) as a function of wavelength is shown in Figure 3. (Sn_{1-x}Cu_xO₂). As the concentration of (Copper oxide) increases, the absorbance drops. The increase in absorbance can be linked to the increase in lattice defect and, as a result, the increase in absorption.

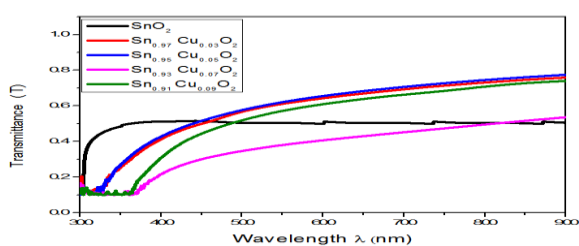


Figure (2), Transmittance for (Sn_{1-x}Cu_xO₂) where (x= 0, 0.03, 0.05, 0.07 and 0.09)

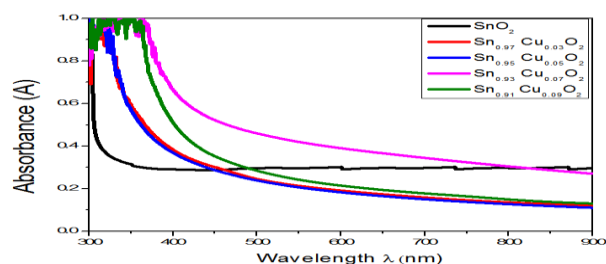


Figure 3: Absorbance spectra of (Sn_{1-x}Cu_xO₂) where (x= 0, 0.03, 0.05, 0.07 and 0.09).

The absorption coefficient is estimated by [8- 14]:

$$\alpha = \frac{2.303 \cdot A}{t} \quad (5)$$

Where: A is absorbance, t is the thickness of films and (α) is the absorptions coefficient. Figure (4) indicates that in the visible range of the spectrum, all films have higher absorption coefficients. Copper oxide level increased, and the coefficient absorption decreased at random. The position of the absorption edge shifts somewhat throughout the figure, which could be caused to Cu atoms that limit the growth of SnO₂ grains. [4]

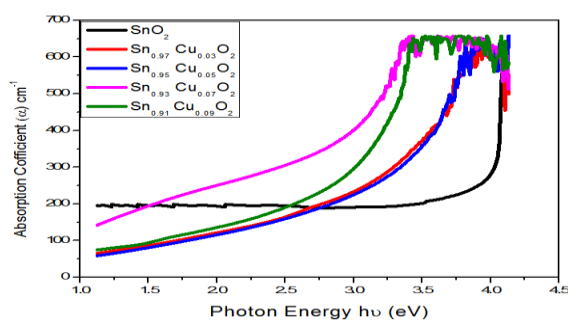


Figure 4: Absorption coefficient versus Wavelength of (Sn_{1-x}Cu_xO₂) where (x= 0, 0.03, 0.05, 0.07 and 0.09)

The optical band gaps is evaluated by [14]:

$$ahv = B(hv - E_g)^r \quad (3)$$

Where: α is the absorption coefficient, hv is the energy of photon, and B is the constant independent of photon energy. r=1/2 for direct transitions. As illustrated in Figure, the optical band gap values were calculated by drawing a straight line from (hv)²=0 to (hv)²=0. As demonstrated in figure (5), the band gap values fell as the copper oxide content rose, owing to the dissimilarity of the mixed phase film. [4], as well as crystallite size, are responsible for the gap difference. [7]



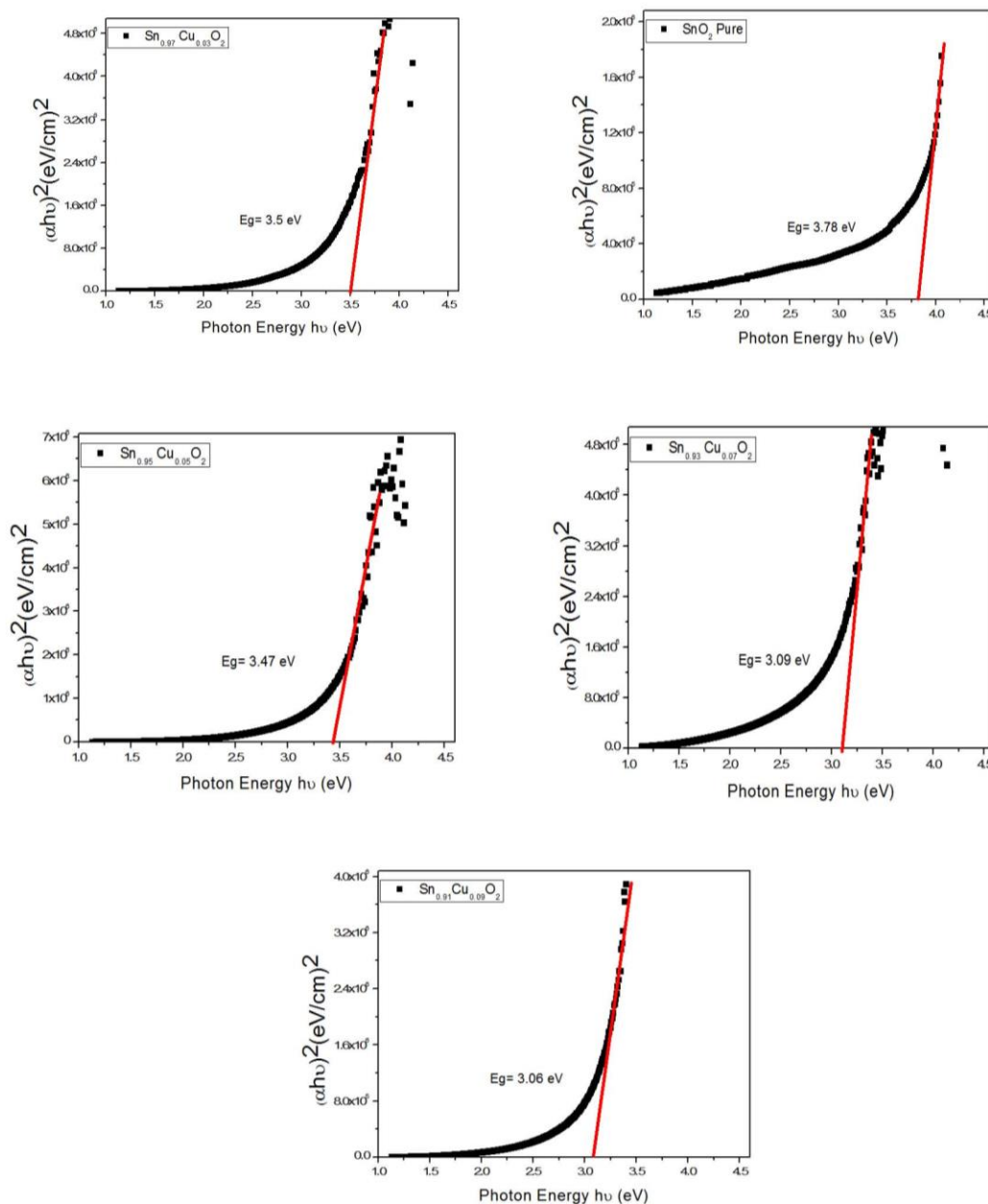


Figure 5: Tauc’s plot of (Sn_{1-x}Cu_xO₂) films where (x= 0, 0.03, 0.05, 0.07 and 0.09)

The extinction coefficient (K_o) was calculated using relation [6, 15]:

$$K_o = \frac{\alpha\lambda}{4\pi} \tag{6}$$

Where K_o : extinction coefficient and λ : wavelength of photon incident. Figure (6) depicts the relationship between wavelength and extinction coefficient in thin films with varying copper oxide ratios. At short wave lengths (300-450) nm, the extinction coefficient (K_o) drops fast

before becoming constant. When the Copper oxide ratio rises, the value of K_o rises as well.



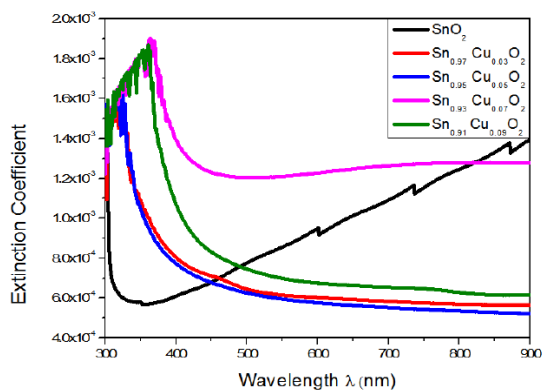
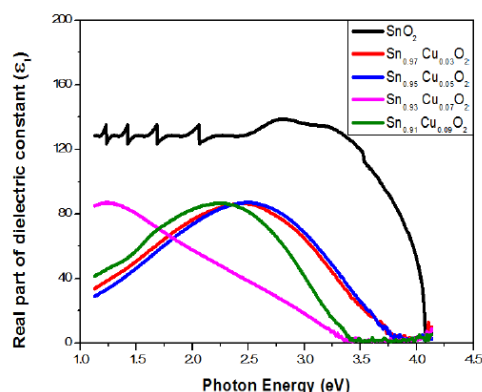


Figure 6: Extinction coefficient against wavelength of (Sn_{1-x}Cu_xO₂) thin films

where (x= 0, 0.03, 0.05, 0.07 and 0.09

The constant of the dielectric can be estimated by using [7, 15]:



$$\epsilon = \epsilon_1 - i\epsilon_2 \tag{7}$$

Where (ϵ_1) Where 1 denotes the real part of the complex dielectric constant and (ϵ_2) denotes the imaginary part. The following formulas can be used to determine the dielectric constant in its two parts:

$$\epsilon_1 = n^2 - K_o^2 \tag{8}$$

$$\epsilon_{12} = 2 n K_o \tag{9}$$

Where (n) is the refractive index. Figure (7) depicts the relationship between real and imaginary parts of the dielectric constant and photon energy for films of various ratios of Copper oxide, with increasing photon energy and ratios of Copper oxide, both the imaginary and real parts of the dielectric constant decrease.

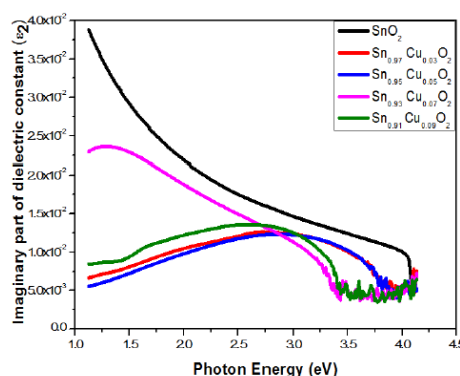


Fig. (7) Imaginary and real parts of dielectric constant for (Sn_{1-x} Cu_xO₂) thin films where (x= 0, 0.03, 0.05, 0.07 and 0.09

4. Conclusions

Sn_{1-x}Cu_xO₂ films were synthesized using the chemical spray pyrolysis method at (x = 0, 0.03, 0.05, 0.07, and 0.09). The samples generated undoped SnO₂ and copper oxide polycrystalline with a tetragonal structure, according to XRD analysis. As the copper oxide content grew, the band gap shrank. Controlling the development of the films by adjusting the temperature and spraying time.

5. REFERENCES

1. Lu, Y. (2015). *SnO₂ thin films-chemical vapor deposition and characterization* (Doctoral dissertation, Gießen, Justus-Liebig-Universität, Diss., 2015).
2. Gaddari, A., Amjoud, M., Berger, F., Sanchez, J. B., Lahcini, M., Rhouta, B., ... & Mavon, C. (2013). *SnO₂ thin films used as ammonia sensing layers at room temperature*. In MATEC Web of Conferences (Vol. 5, p. 04010). EDP Sciences.
3. Mahmood, S. S., & Hasan, B. A. (2019). *Effect of Dopant Concentration on the Structural, Optical and Sensing Properties of (SnO₂)_{1-x}*



- $x(\text{TiO}_2:\text{CuO}_x)$ Sprayed Films. Baghdad Science Journal, 16(2).
4. Habubi, N. F., Oboudi, S. F., & Chiad, S. S. (2012). *Study of some optical properties of mixed $\text{SnO}_2\text{-CuO}$ thin films.*
 5. Hassan, K. H., Saadi, S. K., Jarullah, A. A., & Harris, P. (2018). *Green synthesis and structural characterisation of CuO nanoparticles prepared by using fig leaves extract.* Pakistan Journal of Scientific & Industrial Research Series A: Physical Sciences, 61(2), 59-65.
 6. Ziad T. Khodair, Noor M. Ibrahim, Talib J. Kadhim, Ali M. Mohammad (2022). *Synthesis and characterization of nickel oxide (NiO) nanoparticles using an environmentally friendly method, and their biomedical applications.* Chemical Physics Letters, 797(139564), 1-6.
 7. Khodiar, Z. T., Habubi, N. F., Abd, A. K., & Shano, A. M. (2020). *Structural and Morphological Properties of $\text{Cu}_{1-x}\text{Al}_x\text{O}$ Nanostructures Prepared by sol-gel Method.* Int. J. Nanoelectron. Mater., 13(3), 433-444.
 8. Ahmed, M. S., Iftikhar, M. A., & Nabeel, A. B. (2019). *Photodetector properties of polyaniline/cuo nanostructures synthesized by hydrothermal technique.* 11, 06016(6pp)
 9. Ali, I. M., Shano, A. M., & Bakr, N. A. (2018). *H₂S gas sensitivity of PANi nano fibers synthesized by hydrothermal method.* Journal of Materials Science: Materials in Electronics, 29(13), 11208-11214.
 10. Ziad T. Khodair, Anees A. Khadom, and Hassan A. Jasim. (2019). *Corrosion protection of mild steel in different aqueous media via epoxy/nanomaterial coating: preparation, characterization and mathematical views.* J. Mater. Res. Technol. Vol.8, No. 1, pp. 424-435.
 11. Ziad T. Khodair, Mushtaq A. Al-Jubbori, Ahmed M. Shano, and Fadhil I. Sharrad. (2020). *Study of Optical and Structural Properties of $(\text{NiO})_{1-x}(\text{CuO})_x$ Nanostructures Thin Films.* Chem. Data Collect, Vol.28, p. 100414.
 12. Bakr, N. A., Salman, S. A., & Shano, A. M. (2015). *Effect of co doping on structural and optical properties of NiO thin films prepared by chemical spray pyrolysis method.* International Letters of Chemistry, Physics and Astronomy, 41, 15-30.
 13. M. M. Farhan, Z.T. Khodair and B.A. Ibrahim. (2020) *.Study of the Structural and Optical Properties of Ni-doped Co_3O_4 Thin Films Using Chemical Spray Pyrolysis Technique,* IOP Conf-Series: Materials Science and Engineering 871, 012090.
 14. Khudhur, A. M., Shano, A. M., & Abbas, A. S. H. (2021, September). *A New Neuron Ion Channel Model Under Time Varying Input Currents.* In Journal of Physics: Conference Series (Vol. 1999, No. 1, p. 012127). IOP Publishing.
 15. Z. T. Khodair, N. A. Bakr, A. M. Hassan, A. A. Kamil.(2019). *Influence of substrate temperature and thickness on structural and optical properties of CZTS nanostructures thin films.* J. Ovonic Res. Vol. 15, No. 6, p. 377 – 385.

